Phenotype and Functional Characterization of Long-term gp100-Specific Memory CD8$^+$ T Cells in Disease-Free Melanoma Patients Before and After Boosting Immunization

Edwin B. Walker,[1] Daniel Haley,[1] Ulf Petrausch,[1] Kevin Floyd,[1] William Miller,[1] Nelson Sanjuan,[1] Greg Alvord,[2] Bernard A. Fox,[1] and Walter J. Urba[1]

Abstract

Purpose: Effective cancer vaccines must both drive a strong CTL response and sustain long-term memory T cells capable of rapid recall responses to tumor antigens. We sought to characterize the phenotype and function of gp100 peptide-specific memory CD8$^+$ T cells in melanoma patients after primary gp100$_{209\text{-}2M}$ immunization and assess the anamnestic response to boosting immunization.

Experimental Design: Eight-color flow cytometry analysis of gp100-specific CD8$^+$ T cells was done on peripheral blood mononuclear cells collected shortly after the primary vaccine regimen, 12 to 24 months after primary vaccination, and after boosting immunization. The anamnestic response was assessed by comparing the frequency of circulating gp100-specific T cells before and after boosting. Gp100 peptide-induced *in vitro* functional avidity and proliferation responses and melanoma-stimulated T-cell CD107 mobilization were compared for cells from all three time points for multiple patients.

Results: The frequency of circulating gp100-specific memory CD8$^+$ T cells was comparable with cytomegalovirus-specific and FLU-specific T cells in the same patients, and the cells exhibited anamnestic proliferation after boosting. Their phenotypes were not unique, and individual patients exhibited one of two distinct phenotype signatures that were homologous to either cytomegalovirus-specific or FLU-specific memory T cells. Gp100-specific memory T cells showed some properties of competent memory T cells, such as heightened *in vitro* peptide-stimulated proliferation and increase in central memory (T_{CM}) differentiation when compared with T-cell responses measured after the primary vaccine regimen. However, they did not acquire enhanced functional avidity usually associated with competent memory T-cell maturation.

Conclusions: Although vaccination with class I – restricted melanoma peptides alone can break tolerance to self-tumor antigens, it did not induce fully competent memory CD8$^+$ T cells—even in disease-free patients. Data presented suggest other vaccine strategies will be required to induce functionally robust long-term memory T cells.

Previous vaccine trials done primarily in patients with metastatic melanoma showed that the administration of class I – restricted peptides from gp100 (1, 2) and MART-1 (3, 4) resulted in the *in vivo* expansion of functionally attenuated or senescent CD8$^+$ T cells that were unable to induce long-lasting tumor regression (reviewed in refs. 5, 6). These patients had potentially compromised immunity secondary to large tumor burdens, and there were few opportunities to study the long-term antimelanoma memory T-cell response due to poor patient survival. Recent studies suggest that effective vaccine therapy must not only stimulate CTL activity, but must also sustain long-term memory T cells capable of mounting strong proliferative and functional responses to secondary tumor antigen challenge (refs. 7, 8, reviewed in ref. 9). The phenotype and functional characterization of tumor-specific T cells in similarly vaccinated melanoma patients with less advanced disease and potentially more robust immunity may show enhanced T-cell responses and provide a better opportunity to study the activation and maintenance of long-term melanoma-specific memory T cells (10 – 12).

Given the "self" nature of many tumor-associated antigens and the fact that productive antitumor immunity requires some degree of abrogation of self-tolerance, it is reasonable to expect that self-tumor antigen-specific memory T cells may have phenotypes different from those described for T cells specific for common viral antigens, such as cytomegalovirus (CMV) or

Authors' Affiliations: [1]Robert W. Franz Cancer Research Center, Earle A. Chiles Research Institute, Providence Portland Medical Center, Portland, Oregon and [2]Data Management Services, Frederick Cancer Research and Development Center, National Cancer Institute, Frederick, Maryland

Received 1/3/08; revised 4/11/08; accepted 4/11/08.

Grant support: NIH IR21-CS82614-01 (W.J. Urba), NIH RA21-CA099265-02 (W.J. Urba), NIH R01-CA119123 (B.A. Fox), Murdock Charitable Trust, and Chiles Foundation.

The costs of publication of this article were defrayed in part by the payment of page charges. This article must therefore be hereby marked *advertisement* in accordance with 18 U.S.C. Section 1734 solely to indicate this fact.

Note: Supplementary data for this article are available at Clinical Cancer Research Online (http://clincancerres.aacrjournals.org/).

Requests for reprints: Edwin B. Walker, Robert W. Franz Cancer Research Center, Earle A. Chiles Research Institute, Providence Portland Medical Center, 4805 North East Glisan Street, North Pavilion, 2nd Floor, 2N35, Portland, OR 97213. Phone: 503-215-2620; Fax: 503-215-6841; E-mail: Edwin.walker@providence.org.

©2008 American Association for Cancer Research.

doi:10.1158/1078-0432.CCR-08-0022

Downloaded from http://aacrjournals.org/clincancerres/article-pdf/14/16/5270/1975801/5270.pdf by guest on 09 December 2023

FLU peptides. However, recent data also suggest that self-tumor antigen-specific memory CD8+ T cells exhibit phenotypes homologous to CMV peptide-specific T cells—characterized by low CCR7 expression and dominant expression of effector memory (T_{EM}) and effector-like subpopulations (refs. 10, 13, 14, reviewed in refs. 9, 15). The characterization of memory and effector T-cell phenotypes in different tumor and infectious disease models has been limited by the use of three-color and

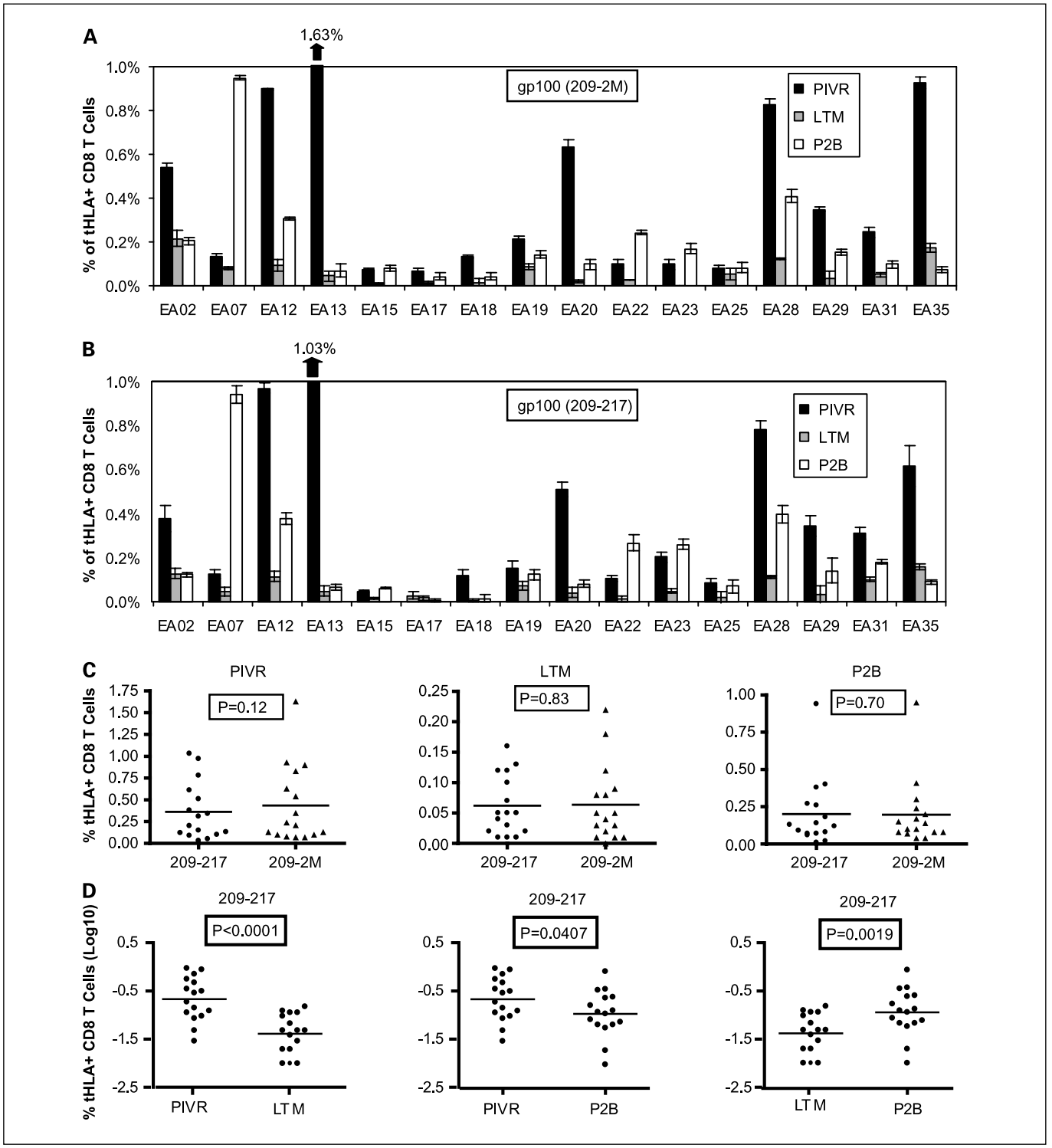

Fig. 1. Boosted P2B PBMCs exhibited an anamnestic increase in the frequency of circulating gp100-specific CD8+ T cells compared with LTM values. Both modified (*A*) and native (*B*) peptide-specific tetramer+ CD8+ T-cell frequencies were >LTM values for 12 of 16 patients, and there was no difference between the mean modified versus native tetramer staining frequencies at each time point (*C*). The mean *ex vivo* gp100209-217 tetramer+ CD8+ T-cell frequency for P2B cells from all patients was significantly higher ($P = 0.0019$) than the mean for LTM cells, but was lower ($P = 0.0407$) than the mean PIVR response for all patients (*D*). Five patients (EA07, EA15, EA22, EA23, EA25) also exhibited boosted P2B tetramer frequencies >PIVR values.

Downloaded from http://aacrjournals.org/clincancerres/article-pdf/14/16/5270/1975801/5270.pdf by guest on 09 December 2023

four-color flow cytometry analysis. The enhanced resolution of higher order (8-10 color) flow cytometry should produce a more comprehensive phenotype characterization of memory T cells and more definitively determine whether or not tumor-specific memory T cells express phenotypes that differ significantly from competent memory T cells specific for common viral antigens.

We previously showed that completely resected patients with stages I to III melanoma vaccinated with the HLA-A2–restricted (modified) melanoma-associated peptide, $gp100_{209\text{-}2M}$, produced significant gp100-specific T-cell responses after 6 months of repetitive vaccination (11, 12). Circulating gp100-specific $CD8^+$ T cells collected 3 to 4 weeks after the last vaccine exhibited high levels of proliferation after *in vitro* stimulation (IVS) with cognate peptide. Native and modified gp100 peptide-loaded A2-restricted MHC class I dimers, as well as $A2^+/gp100^+$ melanoma cell lines, stimulated *ex vivo* production of IFN-γ by these T cells in the majority (>60%) of patients (16). Long-term gp100-specific $CD8^+$ memory T cells, exhibiting high proliferative and functional responses after *in vitro* activation, were detected in the peripheral blood ≥12 months after the last vaccination in the majority of patients. However, the limited numbers of peripheral blood mononuclear cells (PBMC) available prevented a detailed functional or phenotype analysis of these memory T cells. We were also interested in the anamnestic potential of these cells because, as with most infectious agents, long-term immunity to self-tumor antigens may require boosting immunization to maintain adequate numbers of tumor-specific T cells. We therefore sought to study the effect of boosting immunization on patients from our initial trial who were disease-free for at least 1 year after their last gp100 vaccine.

Sixteen patients from the initial trial were given multiple $gp100_{209\text{-}2m}$ boosting immunizations. The frequency of long-term memory gp100-specific $CD8^+$ T cells, and the effect of boosting were assessed by *ex vivo* tetramer analysis. Herein, we describe the eight-color phenotype of gp100 peptide-specific long-term memory and boosted $CD8^+$ T cells and compare the frequency of central memory (T_{CM}), effector memory (T_{EM}), and effector (T_{EFF}) subpopulations at these two time points to frequencies observed 3 to 4 weeks after the initial vaccine regimen was completed. Additionally, these phenotypes were compared with the phenotypes of CMV (pp65) and FLU(M1)-specific memory $CD8^+$ T cells. Correlated functional avidity, proliferation responses, and tumor-specific CD107 mobilization were also compared for gp100-specific $CD8^+$ T cells from all three time points to determine the relative strength of long-term memory functional responses and the effect of boosting immunization on these variables.

Materials and Methods

Patient samples. Thirty-five HLA-$A2^+$ patients with resected stages I to III melanoma were randomized to receive $gp100_{209\text{-}2M}$ peptide in Montanide ISA adjuvant every 2 or 3 wk for 6 mo (11). The HLA-A2-restricted $gp100_{209\text{-}2M}$ peptide (NSC 683472) was provided by the Cancer Therapy Evaluation Program under a National Cancer Institute Investigational New Drug Application (BB6123). A leukapharesis was done before treatment and 1 to 2 wk postcompletion of the initial vaccine regimen (PIVR). Subsequently, 16 of the patients who were disease-free for >12 mo and willing to give informed consent were enrolled in a second booster vaccine trial. Both protocols were reviewed by Cancer Therapy Evaluation Program–National Cancer Institute and approved by the Providence Health System Institutional Review Board. All patients gave their written informed consent before screening for eligibility. Each patient underwent leukapharesis before boosting immunization with the $gp100_{209\text{-}2M}$ peptide in Montinide ISA 51 adjuvant to assess the frequency and functional properties of long-term memory (LTM) T cells. The first two boosting vaccines were given 30 d apart, and a third leukopak was collected 3 wk after the second boosting immunization (P2B). Thereafter, boosting immunization and 50 mL blood collections were done every 6 mo in 3 y. All patients received s.c. injections at two separate sites that totaled 1 mg of peptide and 2 mL of Montanide ISA 51 (11). PIVR, LTM, and P2B cryopreserved PBMCs were used for all *ex vivo* polychromatic flow cytometry studies and IVS expansion cultures.

Interleukin 15/low-dose interleukin-2 IVS. Cryopreserved PIVR, LTM, and P2B PBMCs were stimulated with $gp100_{209\text{-}2M}$ in 7-d IVS cultures in the presence of interleukin-15 (IL-15) and low-dose IL-2, as described previously (12). Cells were thawed and washed twice in Dulbecco's PBS with 2% human AB serum (Irvine Scientific) before being cultured in X-vivo-15 medium (BioWhittaker) with 5% human AB serum. Cells were plated at 12.5×10^5/mL in 200 μL/well in a round-bottomed polystyrene 96-well plate in medium containing $gp100_{209\text{-}2M}$ peptide (0.01 μg/mL), human IL-15 (50 ng/mL; Peprotech), and cultured for 2 d at 37°C in a 5% CO_2 humidified incubator. On day 2, rhIL-2 (PROLEUKIN, Chiron Corporation) was added to provide a final concentration of 60 IU/mL in each culture well. On day 7 of culture, 2 mmol/L EDTA were added to each well for 5 min, cells were harvested and transferred to 5 mL polystyrene tubes and washed thrice in Dulbecco's PBS before functional avidity or CD107 analysis.

Eight-color flow cytometry analysis. Fluorescent antibodies were purchased or fluorescenated in-house with the use of commercially available QDot antibody conjugation kits (Invitrogen, Molecular Probes). The staining panel consisted of the following: CCR7-FITC (R&D Systems), HLA-A2–restricted $gp100_{209\text{-}2M}$ (IMDQVPFSV), and $gp100_{209\text{-}217}$ (ITDQVPFSV) tetramer-PE (iTAg, Beckman Coulter), CD8β-PE-TR, CD28-PE-CY7 (Beckman Coulter), CD14 PE-Cy5 (Beckman Coulter), CD19-PE-Cy5 (eBioscience), CD45RA-APC, strepavidin–APC-CY7 (BD Bioscience, PharMingen), CD57biotin (BD Bioscience, Immununocytometry Systems), and affinity-purified CD27 (BD Bioscience, PharMingen) conjugated to Quantum Dot 605. HLA-A2–restricted FLU $MI_{58\text{-}66}$ (GILGFVFTL) and $CMVpp65_{495\text{-}503}$ (NLVPMVATV) peptide-specific, PE-conjugated tetramers (iTAg, Beckman Coulter) were used in the same eight-color panel to identify FLU-specific and CMV-specific $CD8^+$ T cells. The use of a "dump cocktail" of CD19 and CD14-PE-Cy5 in combination with 5 μg/mL of 7-aminoactinomycin D (Invitrogen, Molecular Probes) in 1 × PBS was used to stain cells with high cell surface Fc receptor–mediated nonspecific binding of antibodies and to discriminate between live and dead cells (17). All data were acquired on a nine-color Dako Cyan ADP flow cytometer equipped with three diode lasers (488, 635, and 407 nm) and modified with optimal bandpass and dichroic filters (Dako). PIVR, LTM, and P2B PBMCs were examined by direct *ex vivo* interrogation of unmanipulated freshly thawed cells using the eight-color staining panel described above. Viable $CD14^-/CD19^-$ lymphocytes were gated for positive CD8β and gp100 tetramer staining, and gp100-specific $CD8\beta^+$ T cells were further interrogated for expression of the remaining five cell-surface markers (CCR7, CD45RA, CD57, CD27, CD28) to determine their subphenotypes. All data were acquired in FCS format (Summit 4.2) and analyzed using Winlist 5.0 Software (Verity House Software). Computer-assisted digital compensation was done using single-color staining controls via the Hyperlog transform (Verity House Software; refs. 18, 19). "Fluorescence minus one" controls were used to set hinged-gating and define histogram regions that distinguished positive from negative events for each fluorescent variable (17, 19, 20). Fidelity controls were used to ensure that there was no loss

Downloaded from http://aacrjournals.org/clincancerres/article-pdf/14/16/5270/1975801/5270.pdf by guest on 09 December 2023

of staining frequency and intensity between lower order panels and the corresponding fluorescence for each monoclonal antibody in the eight-color panel.

Carboxyfluoroscein succinimidyl ester analysis. PBMCs were thawed, washed in Dulbecco's PBS, and pelleted by centrifugation. Cells were resuspended in prewarmed (37°C) Dulbecco's PBS at 50×10^6 cells/mL and loaded with 7 μL of a 0.05 μmol/L working stock of carboxyfluoroscein succinimidyl ester (CFSE) in DMSO (CellTrace, Invitrogen) per 1 mL of cell suspension. After CFSE incubation for 10 min at 37°C staining was quenched by the addition of five volumes of ice-cold culture medium containing 10% human AB serum and incubation on ice for 5 min. Cells were washed thrice in PBS, resuspended at 1×10^6/mL in X-vivo-15 medium supplemented with IL-15 (50 ng/mL), IL-2 (60 IU/mL), and 5% human AB serum and plated at 2.5×10^5 per well (250 μL) in a 96-well plate. Cells were stimulated with 0.0025 μg/well (0.01 μg/mL) of $gp100_{209\text{-}2M}$ peptide for 2 to 7 d. Cells were collected at different time points and stained with anti-CD3 PE-Cy7 (BD Bioscience), CD8 APC-H7 (BD Bioscience), $gp100_{209\text{-}217}$ tetramer APC (iTag, Beckman-Coulter), and Annexin PE (BD Bioscience, PharMingen). CFSE (FITC) staining of pregated viable gp100 tetramer$^+$ CD8$^+$ T cells was analyzed on a DAKO Cyan ADP flow cytometer, and determination of the number of cell divisions from CFSE fluorescence decay data was calculated using ModFit software analysis (Verity House Software).

Data reduction and cluster analysis. FCOM (which stands for "combination function") is a variable in Winlist that can be used to categorize and bin a fluorescent cellular event based on all the combinations of predefined (pregated) fluorescence regions that contain the event. This function uses gated positive regions of multiple fluorescence variables to enumerate cells in all of the possible subphenotypes, as defined by the number of gating variables. The absolute number of gated cells of each defined subphenotype can be assessed and displayed as a discrete peak on the FCOM histogram array. The relative percentage of all cells in each of the subphenotypes are calculated in FCOM and displayed separately (19). Because the number of subphenotypes for any given sample population is a power function (2^n, where n is the number of phenotype gates), FCOM delineated 32 subphenotypes with the five antibodies described in this study. The relative percentages of gp100 tetramer$^+$ T cells with each subphenotype were used for unsupervised cluster analysis. Average-linkage hierarchical clustering was done with the Institute for Genomic Research Multi-Experiment Viewer (TIGR MeV 3.1; refs. 19, 21). Data files generated by FCOM were reformatted to mimic the Affymetrix data file format to accommodate loading into MeV software.

Functional avidity assay: IFN-γ flow cytometry analysis. IFN-γ cytokine flow cytometry functional avidity analysis was done using freshly harvested IVS T cells. 1×10^6 T cells per well were placed in a round-bottomed 96-well plate in 200 μL of X-VIVO-15 medium supplemented with 5% human AB serum (complete medium). Cells were restimulated with $gp100_{209\text{-}2M}$ or $gp100_{209\text{-}217}$ peptide at various concentrations covering a 7-log range (0.00001-10 μg/mL). The cells were incubated 1 h before brefeldin A (Sigma Chemical) was added at 1.25 μg/well (5 μg/mL). Cells were incubated an additional 14 h before they were collected and stained. Twenty-five microliters of 20-mmol/L EDTA were added to each well for 10 min at room temperature to stop the IFN-γ response before collection. Cells were washed twice with 3 mL of staining buffer and suspended in 50 to 100 μL of staining buffer for subsequent fixation, permeabilization, and staining. Cells were fixed in 1 mL of 1 × BD FACS-lysis solution (BD Biosciences) for 10 min at room temperature. All samples were washed in staining buffer and 500 μL of 1 × BD FACS permeabilization solution (BD Biosciences) was added to each tube and incubated at room temperature for 15 min. Permeabilized cells were washed twice, suspended in 50 to 100 μL of staining buffer, and stained with CD3 (FITC)/anti–IFN-γ (PE)/CD8 (PerCP-Cy5.5) monoclonal antibodies (BD Biosciences) before incubation at room temperature for 30 min. After staining, cells were washed twice in staining buffer, fixed in 250 μL of 1% paraformaldehyde (Electron Microscopy Sciences), and stored at 4°C in the dark before analysis. Analysis was done within 24 h of staining. Cells were acquired through a standard lymphocyte light scatter gate (90° versus forward angle), and 5×10^4 to 1×10^5 gated CD8$^+$/CD3$^+$ T cells were analyzed for IFN-γ staining using a FACS Calibur flow cytometry system and CellQuest software (BD Biosciences). Net frequencies of IFN-γ$^+$ cells were calculated by subtracting background "no antigen" (media only) values from the frequency of IFN-γ$^+$ CD8$^+$ T cells after $gp100_{209\text{-}2M}$ peptide stimulation. Data were analyzed with Prism 4.0 (GraphPad Software, Inc.). EC_{50} values were obtained from nonlinear sigmoidal dose-response curves (variable slope, four variables), and the P value was given when two curves were compared side by side.

CD107a/b functional assay. CD107a/b functional analysis was done using freshly harvested IVS T cells. 1×10^6 IVS cells were added to 1-mL cultures in complete medium in a six-well plate. They were stimulated with 0.25×10^6 Mel 118 (A2$^+$/gp100$^+$) or the negative control, Mel 103(A2$^+$/gp100$^-$), melanoma tumor cells per well in the presence of 2 μL of CD107a/b monoclonal antibody (PE) and 1 μL 1,000× monensin (eBioscience) in each well. Cultures were incubated at 37°C for 6 hours after which cells were incubated with EDTA for 10 min at room temperature before they were transferred to staining tubes. Cells were washed twice with 3 mL of staining buffer before staining with $gp100_{209\text{-}2M}$ tetramer (APC) for 1 h at room temperature in the dark. Cells were again washed twice with staining buffer and subsequently stained with CD3 (FITC), and CD8 (PerCP-CY5.5) monoclonal antibodies for 30 min at 4°C. Cells were washed twice in staining buffer, fixed in 250 μL of 1% paraformaldehyde, and stored at 4°C before analysis within 24 h. Cells were analyzed on a FACS Calibur using CellQuest software. Gating and acquisition were as described for the functional avidity assay—1×10^4 to 2×10^4 CD8$^+$/CD3$^+$/tetramer$^+$ T cells were analyzed for the frequency of CD107a/b expression. Background CD107a/b expression stimulated by the negative control cell line Mel 103 was subtracted from the response induced by Mel 118.

Statistical analysis. Data in this study were evaluated using standard descriptive and graphical methods, nonlinear regression analyses, paired parametric and nonparametric tests, hierarchical clustering, and heatmap construction techniques. Tests of significance and four-variable logistic nonlinear regression comparative analyses were done using Prism 4.0 (GraphPad Software, Inc.) and independently confirmed with the R Statistical Package, version 2.5.1 (R Development Core Team, R: a language and environment for statistical computing, R Foundation for Statistical Computing, Vienna, Austria, 2007[3]). Hierarchical and alternative clustering algorithms were computed with and associated heatmaps were constructed with the Institute for Genomic Research Multiexperiment Viewer (TIGR MeV 3.1)[4] (21) and independently confirmed with the R Statistical Package and Bioconductor, version 1.9.9 (22). Two-sided probability values are reported for all tests of significance.

Results

Boosting immunization stimulates anamnestic proliferation of gp100-specific long-term memory T cells. Figure 1A shows the *ex vivo* frequency of $gp100_{209\text{-}2M}$ tetramer-specific CD8$^+$ T cells for PIVR, LTM, and P2B PBMCs from all 16 boosted patients. The frequency range of gp100-specific LTM CD8$^+$ T cells in all patients (0.02-0.2%) was comparable with the frequency ranges of memory T cells specific for FLU (0.06-0.2%) and CMV (0.05-0.5%) antigens in the same patients. Boosted PBMCs showed evidence of a recall response with gp100-specific T-cell

[3] http://www.R-project.org
[4] http://www.tm4.org

Downloaded from http://aacrjournals.org/clincancerres/article-pdf/14/16/5270/1975801/5270.pdf by guest on 09 December 2023

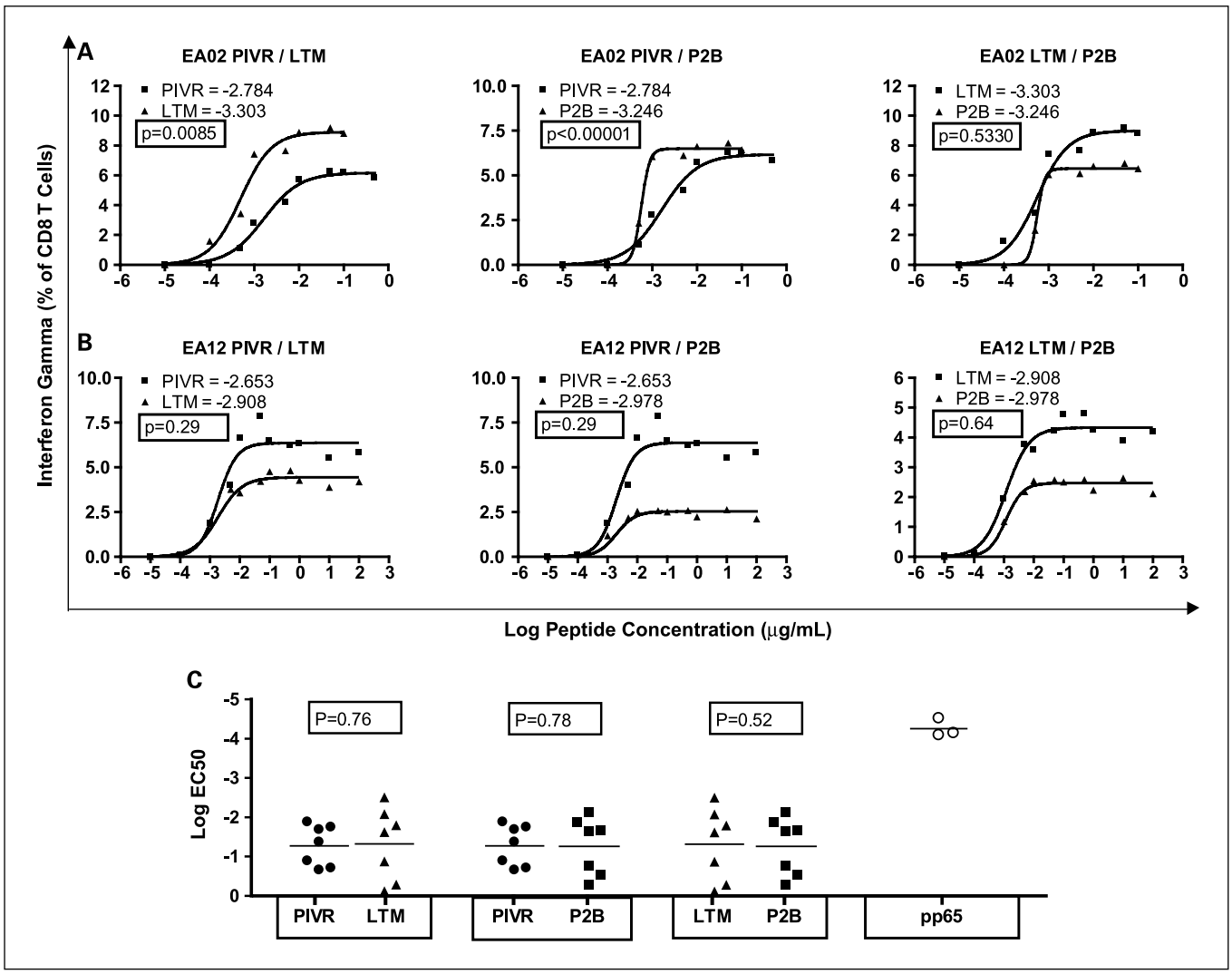

Fig. 2. Comparison of functional avidity for PIVR, LTM, and P2B gp100-specific $CD8^+$ T cells. Cytokine flow cytometry analysis of IFN-γ expression by IVS $CD8^+$ T cells after restimulation with gp100209-2M peptide. EC_{50} values were calculated as an index of functional avidity. CFC (IFN-γ) response curves and EC_{50} values for two patients show that LTM and P2B T cells exhibited significantly higher functional avidity than PIVR cells in some patients (*A*), but not in others (*B*). The cumulative mean log EC_{50} value for all LTM responses was not significantly higher than the mean PIVR value ($P = 0.76$) nor did boosting increase the mean P2B log EC_{50} above the LTM value ($P = 0.52$)—indicating no significant average increase in the functional avidity of LTM or boosted T cells (*C*).

frequencies of 1.5 to ≥20-fold higher than corresponding LTM values in 12 of 16 patients (mean, 6.2-fold increase). However, boosted responses equaled or exceeded PIVR values in only 5 of 16 patients. Comparable frequencies were observed in most patients when native peptide ($gp100_{209-217}$) tetramers were used (Fig. 1B). Paired *t* test analysis showed tetramer binding was not statistically different for the modified and the native peptide at each time point (Fig. 1C). Mean cumulative frequencies of boosted T cells for both peptides were significantly higher than the mean frequencies of long-term memory cells ($P = 0.0019$, native peptide) but were significantly lower than the mean PIVR frequencies at the end of the priming immunization ($P = 0.0407$, native peptide; Fig. 1D). The frequency of circulating gp100-specific $CD8^+$ T cells did not increase beyond P2B levels for the majority of patients (15 of 16) after six more boosting immunizations over 3 years (data not shown). The absence of a more robust secondary response in the peripheral blood could reflect the trafficking of cells to lymph nodes and peripheral tissues as described in infectious disease models (23).

Gp100-specific LTM and P2B T cells do not exhibit enhanced functional avidity. Maturation of memory T cells, characterized by increased functional avidity and cytokine secretion after boosting immunization, has been described (refs. 24–29, reviewed in ref. 30). To determine if long-term memory or boosted T cells exhibited increased functional avidity, PIVR, LTM, and P2B cells were stimulated with low-dose $gp100_{209-2M}$ peptide (0.01 μg/mL) and cultured in IL-15 + low-dose IL-2 for 7 days. Functional avidity was determined by titrating the modified and native gp100 peptide against IVS cells in a standard cytokine flow cytometry (IFN-γ) assay. Nonlinear regression analysis was done, and EC_{50} values were calculated to compare functional avidity. Figure 2A and B shows the response curves and EC_{50} values for PIVR versus LTM, PIVR versus P2B, and LTM versus P2B IVS cells from two of seven patients studied. EA02 (Fig. 2A) LTM cells had a higher

Downloaded from http://aacrjournals.org/clincancerres/article-pdf/14/16/5270/1975801/5270.pdf by guest on 09 December 2023

functional avidity than PIVR cells, and boosting sustained the higher avidity (i.e., LTM = P2B > PIVR). By comparison, the functional avidity of T cells from EA12 was the same at all three time points, suggesting that functional enhancement of LTM and P2B cells had not occurred (Fig. 2B). Overall, there was no statistical difference between the mean cumulative (i.e., for all patients studied) native peptide-induced EC_{50} values for PIVR versus LTM ($P = 0.76$) or between LTM and P2B ($P = 0.52$) by paired t test analysis (Fig. 2C). Similarly, the mean $gp100_{209\text{-}2M}$ stimulated EC_{50} values for all patients at all three time points were not statistically different, although the modified peptide stimulated average EC_{50} values that were 1 to 1.5 logs lower than those stimulated by the native peptide, indicating higher functional avidity for the modified peptide (data not shown). Thus, on average, the functional avidity of LTM $CD8^+$ T cells from seven patients did not exhibit functional enhancement compared with PIVR T cells, and boosting immunization did not improve T-cell functional avidity. To compare the relative strength of the functional avidity of native peptide-induced responses at all time points to that induced by a common infectious disease antigen, we measured the response of CMV ($pp65_{495\text{-}503}$) peptide-induced IVS cells to restimulation with the cognate pp65 peptide. As shown in Fig. 2C, the log of the mean EC_{50} peptide concentration for gp100 was 3 logs higher than the mean EC_{50} value for CMV pp65, indicating a significantly lower avidity for the self-tumor antigen-specific memory T cells.

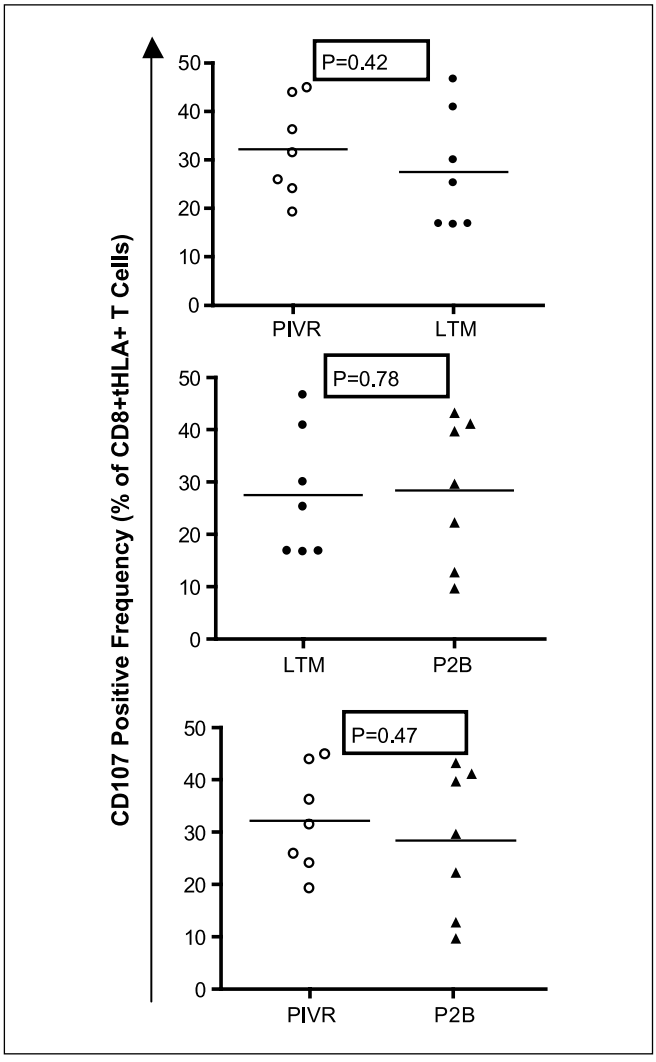

Fig. 3. Comparative CD107 mobilization analysis of PIVR, LTM, and P2B-derived gp100-specific $CD8^+$ T cells from seven patients after *in vitro* challenge with an $A2^+/gp100^+$ melanoma tumor cell line, Mel 118. The mean frequency of LTM $tetramer^+$ $CD8^+$ IVS T cells expressing CD107 was not significantly higher than the mean PIVR $CD107^+$ staining frequency ($P = 0.42$), and boosting immunization did not increase the mean P2B $CD107^+$ frequency above LTM levels ($P = 0.78$). Background CD107 staining induced by the $A2^+/gp100^-$ negative control melanoma cell line, Mel 103, was subtracted from Mel 118 stimulated values.

Melanoma cells stimulate CD107 mobilization by gp100-specific T cells. CD107 cell surface expression has been correlated with perforin and granzyme B degranulation after CTL activation (31). PIVR, LTM, and P2B IVS cells from seven patients were stimulated *in vitro* with an $A2^+/gp100^+$ melanoma cell line, Mel 118, and an $A2^+/gp100^-$ negative control melanoma cell line, Mel 103. CD107 expression was measured in a 6-hour assay, and the net CD107 response was calculated after subtracting the background Mel 103-induced CD107 fluorescence. A no antigen control culture was also run to determine if melanoma cell activation of T cells induced concomitant down-regulation of TCR-specific tetramer staining. There was no statistical difference in the frequency of $tetramer^+$ $CD8^+$ T cells between the no antigen control and Mel 118–stimulated T cells ($P = 0.1557$). The mean frequency of $CD107^+$ $tetramer^+$ $CD8^+$ LTM T cells for all seven patients was not statistically different from the mean frequency measured in PIVR samples, indicating no increase in the frequency of degranulating LTM compared with PIVR tumor-specific T cells, as shown by paired t test analysis ($P = 0.42$; Fig. 3). The same statistical analysis also showed that the mean frequency of P2B $CD107^+$ T cells was not significantly different from the mean LTM value, indicating that boosting immunization did not increase the fraction of gp100-specific $CD8^+$ T cells that responded to tumor cells by degranulation ($P = 0.78$; Fig. 3).

Gp100 peptide stimulates rapid* in vitro *proliferation of LTM $CD8^+$ T cells. ModFit analysis of the loss of CFSE fluorescence by labeled cells from all three time points for patient EA07 stimulated in a gp100 IVS culture illustrates the rapid proliferation kinetics of LTM gp100-specific T cells observed in many patients. As shown in Fig. 4A, by 48 hours, twice as many LTM gp100-specific T cells (43.9%) had divided > 6 times compared with peptide-specific PIVR (20.9%) or P2B T cells (15.1%). PIVR, LTM, and P2B cells from all 16 patients were similarly stimulated *in vitro* with low-dose (0.01 μg/mL) $gp100_{209\text{-}2M}$ for 7 days in the presence of IL-15 and low-dose IL-2, and proliferation was assessed by measuring the frequency of $gp100_{209\text{-}2M}$ $tetramer^+$ $CD8^+$ T cells and calculating the proliferative fold-increase over the *ex vivo* tetramer frequency at each time point. There was minimal antigen-induced apoptosis and cell death of $CD8^+$ T cells during the 7-day culture (data not shown). Several patients (EA15, EA17, EA18, EA25) had low *ex vivo* $tetramer^+$ frequencies (Fig. 1A), and their $CD8^+$ T cells did not proliferate *in vitro* as shown by their low fold-increase values (Fig. 4). EA02 T cells also had a low proliferation response, although they were moderately $gp100_{209\text{-}2M}$ tetramer-positive (range, 0.2-0.55%; Fig. 1A) at all time points. All other patients showed moderate (8-fold to 25-fold increase) to high (≥50-fold increase) proliferation of $tetramer^+$ $CD8^+$ T cells at all time points. LTM cells from 8 of 16

Downloaded from http://aacrjournals.org/clincancerres/article-pdf/14/16/5270/1975801/5270.pdf by guest on 09 December 2023

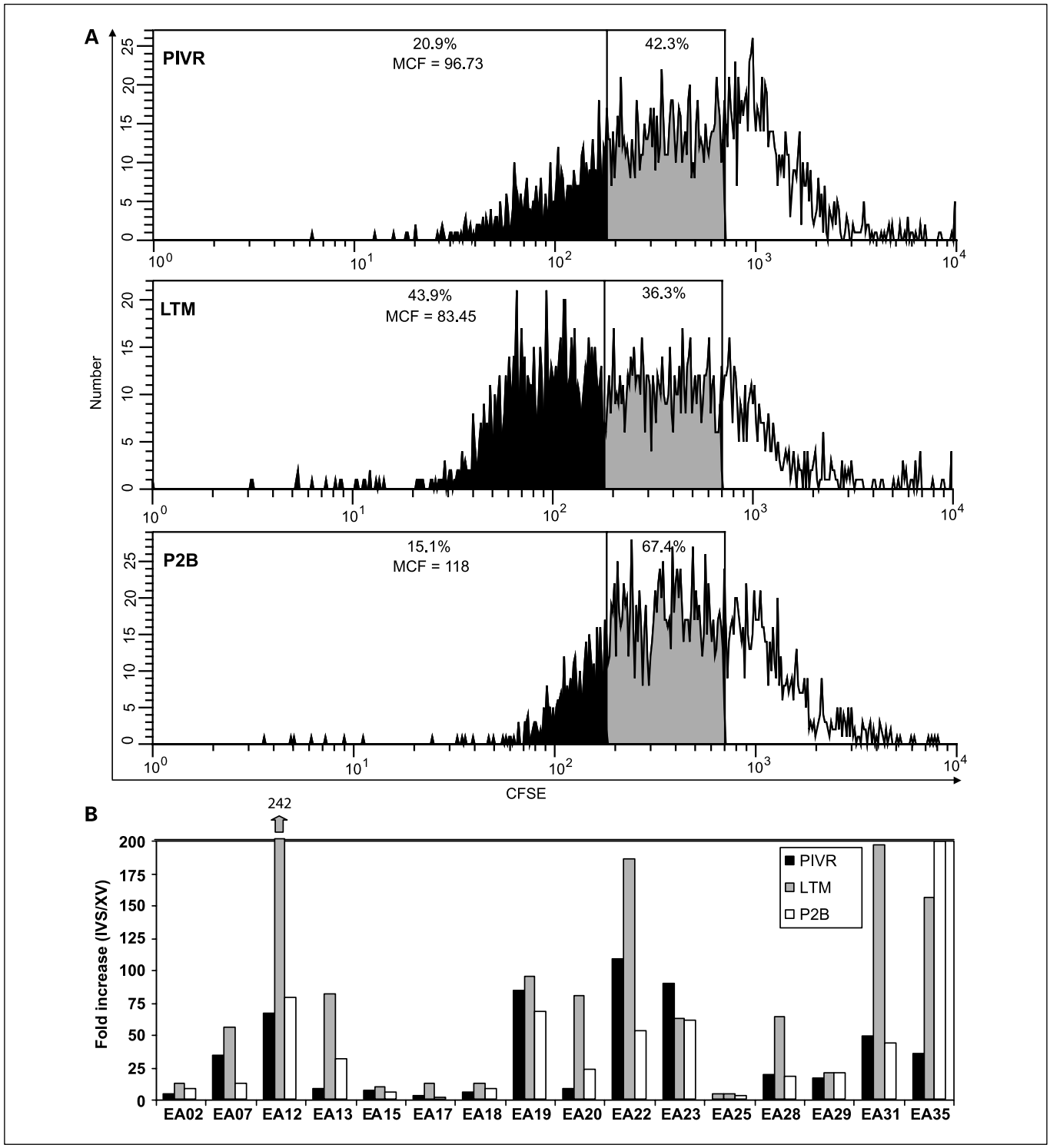

Fig. 4. *In vitro* proliferation of PIVR, LTM, and P2B-derived gp100-specific $CD8^+$ T cells after cognate peptide stimulation. CFSE (FITC) fluorescence decay of gp100 $tetramer^+$ $CD8^+$ T cells from a representative patient after 48 h *in vitro* stimulation with gp100209-2M shows that LTM cells exhibited a very rapid proliferation response resulting in twice the frequency of T cells which doubled > 6 times (43.9%) compared with PIVR (20.9%) and P2B (15.1%) proliferation responses (*A*). Seven-day *in vitro* stimulation of PBMCs with gp100209-2M induced very high fold increases of LTM gp100-$tetramer^+$ $CD8^+$ T cells compared with the fold increase values for corresponding PIVR and P2B cells from 8 of 16 patients (*B*). EA35 exhibited increased proliferation of both LTM and P2B gp100-specific $CD8^+$ T cells compared with PIVR cells.

patients had very high *in vitro* proliferation responses (50-fold to 200-fold increases), which exceeded those observed for their respective PIVR and P2B cells, and equaled or exceeded the IVS fold-increase values for CMV-specific (54.86 ± 9.5) and FLU-specific (60.5 ± 15.1) memory T cells. This suggested they had heightened proliferative capabilities characteristic of competent memory T cells. Similar results were obtained when native peptide was used (data not shown).

Downloaded from http://aacrjournals.org/clincancerres/article-pdf/14/16/5270/1975801/5270.pdf by guest on 09 December 2023

Eight-color flow cytometry delineates multiple memory and effector T-cell subpopulations. Eight-color flow cytometry produces a more comprehensive phenotype characterization of memory and effector T cells than standard three-color to four-color analysis. Figure 5 shows the gating and analysis strategy used to resolve tumor antigen-specific T-cell subphenotypes (19). We identified both early T_{EM} ($CCR7^-/CD45RA^-/CD57^-/CD27^+/CD28^+$) and late T_{EM} ($CCR7^-/CD45RA^-/CD57^-/CD27^+/CD28^-$) subpopulations (Fig. 5, $CCR7^-$ panel), as well as T_{CM} ($CCR7^+/CD45RA^-/CD57^-/CD27^+/CD28^+$) phenotypes (Fig. 5, $CCR7^+$ panel) predicted by consensus models based on 3-color to 7-color analysis (9, 32–36). We also delineated previously undescribed memory T-cell subpopulations. Using a four-color analysis, Sallusto and Lanzavecchia first used the term "T_{EMRA}" to designate $CCR7^-/CD45RA^+$ effector-memory $CD8^+$ T cells (37). Figure 5 shows that gp100-specific $CCR7^-/CD45RA^+$ T cells can be further divided into multiple subphenotypes based on staining with CD57, CD27, and CD28 monoclonal antibodies ($CCR7^-$ panel; dot plots 1 and 2). Herein, the T_{EMRA} designation will refer only to the $CCR7^-/CD45RA^+/CD57^-/CD27^+/CD28^{+/-}$ subphenotypes because it describes the reexpression (or retention) of CD45RA on T_{EM} $CD8^+$ T cells before the acquisition of CD57 and concomitant loss of both CD27 and CD28, which characterizes the transition to terminal effector T cells (35, 36). A similar, previously undescribed subphenotype, which expressed CD45RA on the T_{CM} background ($CCR7^+/CD45RA^+/CD57^-/CD27^+/CD28^+$), was also detected ($CCR7^+$ panel; dot plot 1) and will be called T_{CMRA}. Consensus models define this phenotype as unique to naive T cells (9, 32). However, we detected gp100-specific T cells with this phenotype signature only after repetitive gp100 peptide vaccination, suggesting T_{CMRA} T cells are a true antigen-educated memory subpopulation.

Consensus models suggest that terminal effector $CD8^+$ T cells express CD57 (38) and recapitulate CD45RA expression (32, 39). Accordingly, fully differentiated effector T cells should have the following phenotype: $CCR7^-/CD45RA^+/CD57^+/CD27^{+/-}/CD28^-$. T cells with a similar effector-like phenotype (i.e., $CCR7^-/CD45RA^+/CD27^{+/-}/CD28^-$) persist long term in the blood of healthy CMV-seropositive individuals and may be a result of chronic exposure to viral antigens (15, 33, 40, 41). These cells have recently been called "resting vigilant effector" (T_{RVE}) $CD8^+$ T cells, because they are believed to control latent virus expression (15). Effector-like $CD8^+$ T cells with similar T_{RVE} phenotypes were found in the peripheral blood of some gp100-vaccinated melanoma patients and may similarly reflect the sustained exposure to normal melanocyte or micrometastatic melanoma antigens ($CCR7^-$ panel; dot plot 2).

Low frequencies of previously undescribed $CD8^+$ T cells expressing phenotypic traits of both effector cells (i.e., $CCR7^-/CD45RA^{+/-}/CD57^+$) and memory cells (i.e., $CD27^+/CD28^+$) were also identified among LTM PBMCs ($CCR7^-$; dot plots 2 and 4). Although these T cells may comprise T_{EM} cells in transition to effector or T_{RVE}-like cells, they persisted in disease-free melanoma patients 12 to 24 months after any exogeneous exposure to gp100 peptide. A low frequency of T cells with a

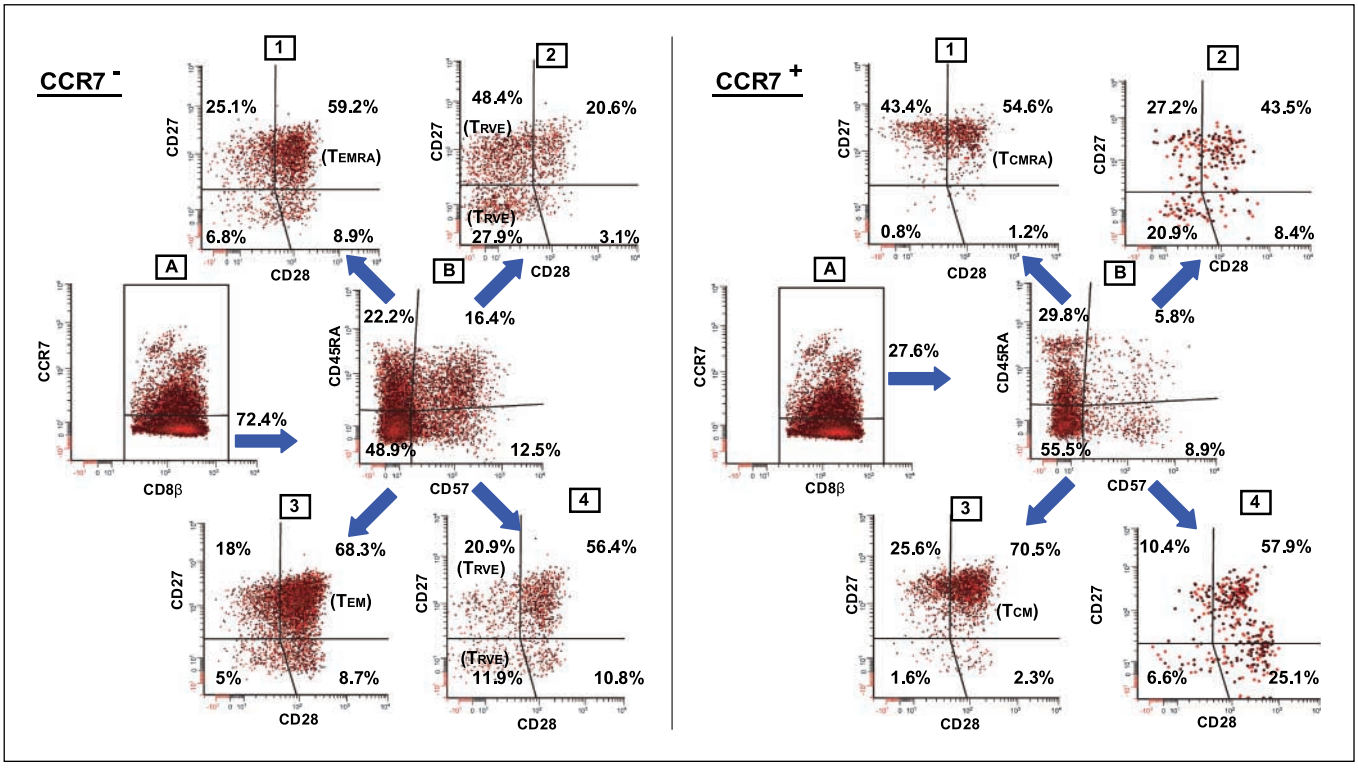

Fig. 5. Sequential two-variable dot-plot gating strategy used for eight-color flow cytometry analysis of gp100-specific $CD8^+$ memory T cells from a representative patient. The staining panel consisted of reagents specific for CD8β/gp100 tetramer/CCR7/CD45RA/CD57/CD27/CD28/CD14, CD19, 7AAD cocktail. Only viable gp100209-217 $tetramer^+$ $CD8^+$ T cells were selected for analysis and further divided into $CCR7^-$ (*left,* dot plot *A*), or $CCR7^+$ (*right,* dot plot *A*) subpopulations. By example, $CCR7^-/tetramer^+/CD8\beta^+$ T cells were selected ($CCR7^-$, dot plot *A*) and further analyzed for CD45RA versus CD57 expression ($CCR7^-$, dot plot *B*). Cells from each of the CD45RA versus CD57 dot plot quadrants were then analyzed for CD27 versus CD28 staining ($CCR7^-$, dot plots 1-4). Sixteen different subphenotypes were delineated in the $CCR7^-$ compartment and, by similar analysis, another 16 subpopulations in the $CCR7^+$ compartment.

Downloaded from http://aacrjournals.org/clincancerres/article-pdf/14/16/5270/1975801/5270.pdf by guest on 09 December 2023

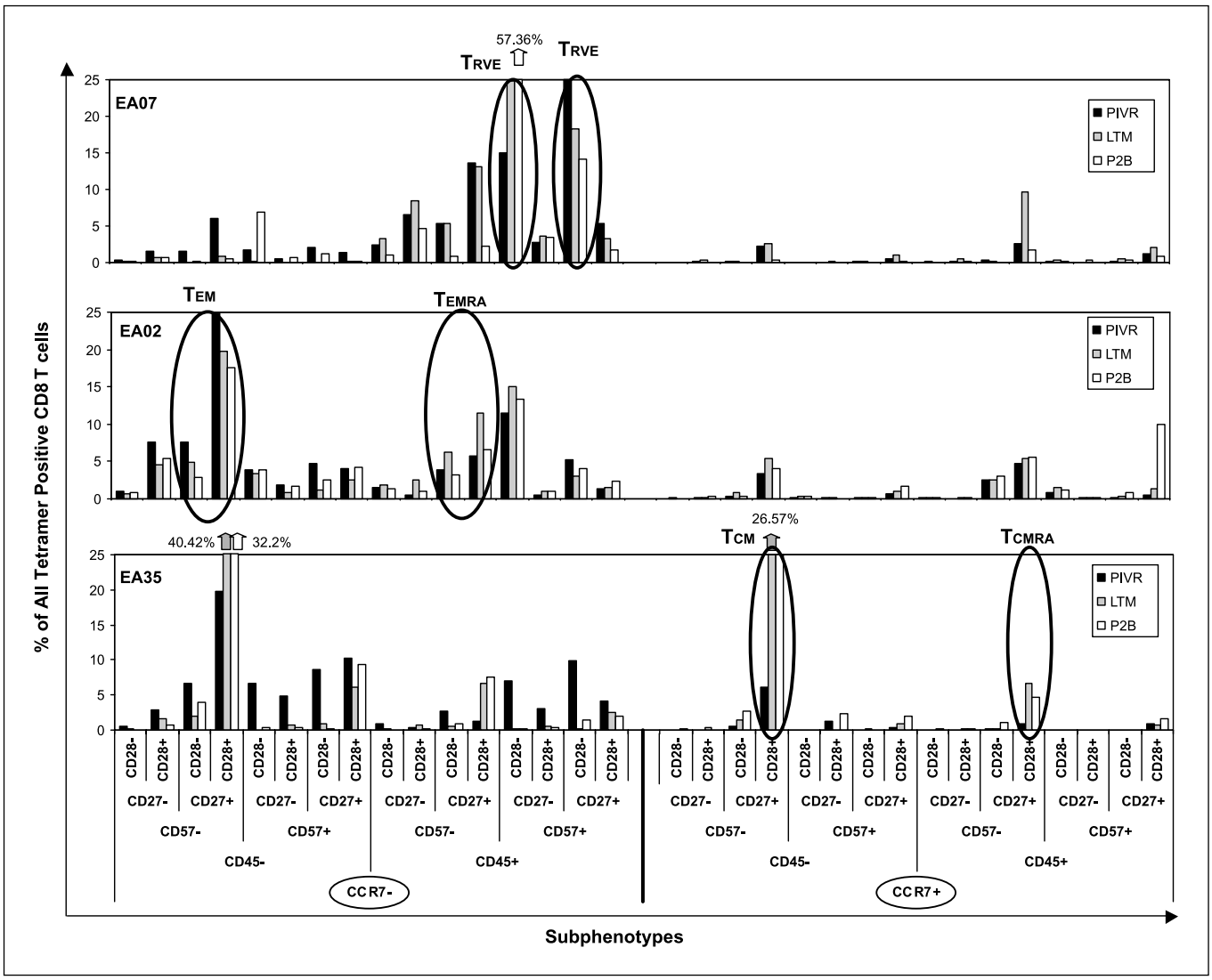

Fig. 6. FCOM generated gp100-specific $CD8^+$ T-cell subphenotype signatures for PIVR, LTM, and P2B PBMCs from three representative patients. The 32 possible subphenotypes of $tetramer^+$ $CD8^+$ T cells are displayed on the *X* axis and are divided into 16 $CCR7^-$ (*left*) and 16 $CCR7^+$ (*right*) subpopulations. Subphenotype signatures are based on the combined positive and negative staining patterns for CD45RA/CD57/CD27/CD28 monoclonal antibodies on PIVR, LTM, and P2B T cells within each CCR7 compartment. Each CCR7 staining compartment is subdivided into $CD45RA^-$ and $CD45RA^+$ subsets, and each CD45RA subpopulation is then further divided into $CD57^-$ and $CD57^+$ T cells. Final subphenotype delineation is defined by positive or negative expression of CD27 and CD28 on T cells in each CD57 subpopulation. Key dominant subphenotypes are designated for clarity of interpretation.

similar phenotype ($CCR7^+$/$CD45RA^{+/-}$/$CD57^+$/$CD27^+$/$CD28^+$) was also seen in the $CCR7^+$ compartment ($CCR7^+$ panel; dot plots 2 and 4). Thus, the more comprehensive phenotype signatures produced using eight-color analysis confirmed the T_{EM} and T_{CM} phenotypes predicted from consensus models, expanded the phenotype characterization of previously described T_{EMRA} and T_{RVE} $CD8^+$ T cells, and delineated previously undescribed subphenotypes, such as T_{CMRA} and putative "transitional" subpopulations with phenotype traits of both effector and memory T cells.

FCOM analysis generated detailed subphenotype signatures of gp100-specific $CD8^+$ T cells. Efficient analysis of potentially different T-cell subpopulations between individual test samples was complicated by the fact that eight-color flow cytometry generated a large amount of data (32 subphenotypes) for each sample. Data reduction and analysis methods, such as FCOM (19), were used to facilitate comparison of phenotypes between PIVR, LTM, and P2B samples within and between patients. Figure 6 shows bar graphs of the frequencies of all 32 FCOM subphenotypes after *ex vivo* analysis of PIVR/LTM/P2B cells from three patients using the aforementioned eight-color staining panel. There were significant interpatient differences, both qualitatively and quantitatively, in the subphenotype frequency distribution pattern (signature) of gp100 $tetramer^+$ $CD8^+$ T cells. Whereas the frequency of $tetramer^+$ $CD8^+$ T cells in each subphenotype varied over the three time points for an individual patient, the qualitative subphenotype signature of antigen-specific cells remained uniform for each patient at all three time points, suggesting it was imprinted at the time of initial antigen exposure. The signatures of all three patients were distinct because of significant differences in the frequency of T_{EM}, T_{CM}, and T_{RVE}/effector subpopulations. Most of the

Downloaded from http://aacrjournals.org/clincancerres/article-pdf/14/16/5270/1975801/5270.pdf by guest on 09 December 2023

gp100-specific $CD8^+$ T cells from patient EA07 were distributed in three major subsets, T_{EMRA} ($CCR7^-/CD45RA^+/CD57^-/CD27^+/CD28^+$) and two dominant T_{RVE} subpopulations ($CCR7^-/CD45RA^+/CD57^+/CD27^-/CD28^-$ and $CCR7^-/CD45RA^+/CD57^+/CD27^+/CD28^-$, respectively). The LTM $CD27^-/CD28^-$ T_{RVE} subpopulation was almost 2-fold higher compared with the PIVR value, and boosting increased its frequency almost 4-fold above PIVR. There were very low percentages of T_{EM} and T_{CM} at all three time points; T_{CMRA} frequencies were low at PIVR and P2B but increased to 10% at LTM. The EA07 gp100-specific T-cell signature was composed of predominantly T_{RVE}-like cells similar to the memory $CD8^+$ T cells found in CMV^+ patients (15). By comparison, the signature for EA02 was characterized by significantly higher T_{EM} frequencies at all three time points. However, similar to EA07, there was a significant T_{EMRA} subpopulation (5-12%), and the second largest subpopulation was the T_{RVE} phenotype (11-15%).

T cells from EA35 were very different than those of EA02 and EA07. The two dominant subpopulations were T_{EM} and T_{CM} cells; there were significant increases in the frequencies of these subpopulations among LTM and P2B gp100-specific T cells compared with PIVR. The EA35 LTM and P2B T_{EM} and T_{CM} frequencies were also significantly elevated compared with those of EA02 and EA07. The EA35 T-cell signature indicated that the higher LTM frequencies of T_{CM} and T_{EM} $CD8^+$ T cells were sustained after boosting immunization. Notably, EA35 long-term memory and boosted gp100-specific T cells did not include T_{RVE} memory subpopulations. Thus, the three gp100-specific T-cell signatures shown in Fig. 6 suggested one patient had an immune response dominated by T_{RVE} memory cells similar to the memory T cells specific for CMV (EA07), whereas a second patient's immune response was characterized by high frequencies of T_{CM} and T_{EM} $CD8^+$ T cells devoid of T_{RVE} expression (EA35). T cells from a third patient (EA02) were characterized by a variation of the T_{RVE} phenotype and exhibited the combined expression of T_{RVE}, as well as T_{EM} memory cells. To determine if other patients expressed these or other memory/effector $CD8^+$ T-cell signatures, direct *ex vivo* analysis of cryopreserved PIVR, LTM, and P2B PBMCs from

Downloaded from http://aacrjournals.org/clincancerres/article-pdf/14/16/5270/1975801/5270.pdf by guest on 09 December 2023

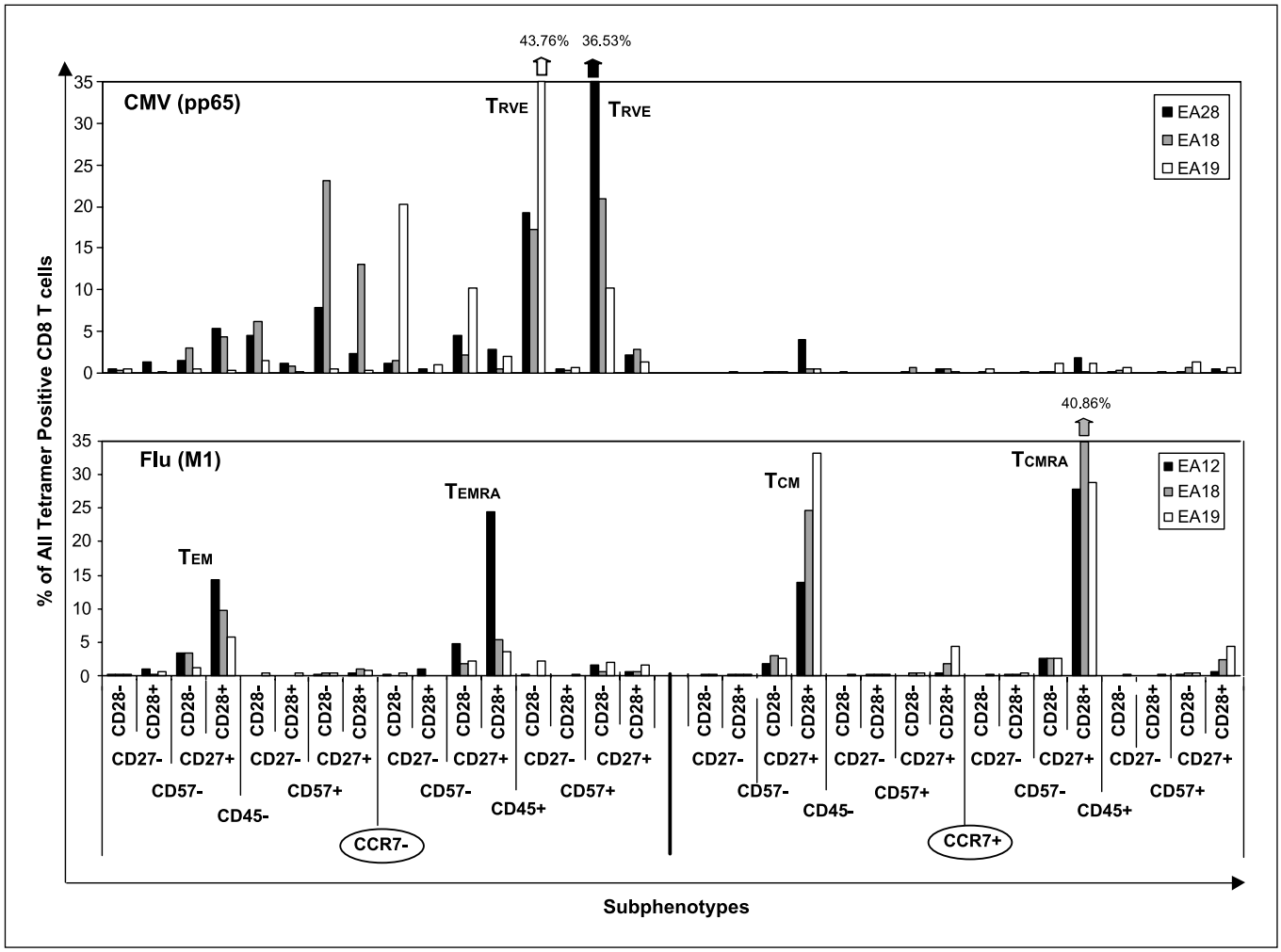

Fig. 7. Eight-color flow cytometry subphenotype signatures of CMV-specific and FLU-specific $CD8^+$ memory T cells. Subphenotypes of CMV (pp65) $tetramer^+$ $CD8^+$ T cells from three patients were all similar and expressed dominant TRVE subpopulations (*top*) characterized by either $CD27^+$ or $CD27^-$ staining on the $CCR7^-/CD45RA^+/CD57^+/CD28^-$ background. FLU (M1) $tetramer^+$ $CD8^+$ T cells from three patients were also homologous, but expressed a distinctly different signature characterized by dominant TEM, TEMRA, TCM, and TCMRA subpopulations and negligible expression of TRVE T cells.

seven other patients was done. Patients were selected because they had enough gp100-specific T cells to ensure the successful acquisition of at least 5×10^3 to 10×10^3 gated gp100 tetramer$^+$ CD8$^+$ T cells required for statistical accuracy of subphenotype delineation. FCOM signatures from all seven patients were compared using unsupervised cluster analysis (Supplementary Fig. S1). Two patients (EA07, EA29) segregated together in a major cluster characterized by dominant T_{RVE} subphenotype expression and low frequencies of T_{EM} and T_{CM} gp100-specific T cells. EA02 was closely associated in a second cluster characterized by high T_{RVE} and T_{EM} subphenotype expression. Four other patients (EA19, EA12, EA28, EA35) segregated together in a third major cluster characterized by cells with dominant T_{CM}, T_{EM}, T_{EMRA}, and T_{CMRA} subphenotypes, but devoid of T_{RVE} subpopulations. Details show that long-term memory and boosted T cells from these four patients had significantly higher frequencies of gp100-specific T_{CM} cells than were detected in PIVR PBMCs (Supplementary Fig. S1). Increased T_{CM} differentiation after antigen depletion represents a memory T-cell maturation trait reported for competent memory T cells in infectious disease models (42–44). Increased T_{CM} expression was only observed in LTM and P2B PBMCs from these four patients—all of whom had memory T-cell signatures similar to those described for memory T cells stimulated by acute viral infection, such as influenza (45, 46).

Gp100-specific T-cell signatures are homologous to those of CMV-specific or FLU-specific memory T cells. To determine if the gp100 peptide-specific T-cell signatures resembled those specific for acute and chronic viral antigens, we used A2-restricted FLU(M1) peptide and CMV (pp65) peptide-specific tetramers in the same eight-color staining panel to phenotype memory T cells from three patients in the trial exposed to CMV and influenza, respectively. The CMV-specific signature was similar for all three patients (Fig. 7). The memory T cells comprised very low frequencies of T_{EM} and T_{EMRA} and very low total frequencies (≤7%) of CCR7$^+$ CD8$^+$ T cells. The two dominant CMV subpopulations were CD27$^-$ and CD27$^+$ effector or T_{RVE}-like phenotypes. By contrast, the FLU-specific memory CD8$^+$ T cells in all three patients shared a different signature; the majority of FLU-specific T cells were in four subpopulations (T_{EM}, T_{EMRA}, T_{CM}, T_{CMRA}), although the frequency of each subpopulation varied between patients. In contrast to CMV, FLU-specific T cells were highly CCR7$^+$—EA12 (46%), EA18 (75.7%), EA19 (76.5%)—and did not include high frequencies of T_{RVE}-like subpopulations (≤5%). The contrast between the signatures of CMV-specific and FLU-specific memory T cells was especially notable in patients EA18 and EA19 because they had memory CD8$^+$ T-cell responses to both viral antigens. The difference between FLU and CMV memory signatures was further confirmed by cluster analysis of a larger number of samples—the signatures for eight CMV samples were very homologous and partitioned separately from the tightly clustered FLU-specific T-cell subpopulations from seven patients (data not shown). Consensus models based on three-color to four-color flow cytometry have suggested memory CD8$^+$ T cells specific for acute viruses, such as influenza, would have a dominant CD45RA$^-$/CCR7$^+$/CD28$^+$/CD27$^+$ phenotype (42, 47), whereas CD8$^+$ memory T cells specific for chronic viruses, such as CMV, would be characterized by a dominant CD45RA$^+$/CD57$^+$/CCR7$^-$/CD27$^-$/CD28$^-$ phenotype (15, 33, 40, 41). Eight-color analysis confirmed these predictions of the consensus models. Additional cluster analysis studies were also done to determine whether gp100-specific CD8$^+$ T-cell signatures for individual melanoma patients segregated with either the FLU-specific or CMV-specific memory T-cell phenotype signatures (Supplementary Fig. S2). The T_{RVE}-rich T-cell signatures of patients EA02, EA07, and EA29 clustered exclusively with the eight CMV-specific CD8$^+$ T-cell signatures (Supplementary Fig. S2A). Conversely, the four patients with very low T_{RVE} subphenotype expression, but high dominant T_{CM}, T_{EM}, T_{EMRA}, T_{CMRA} subpopulations (EA12, EA19, EA28, EA35), clustered exclusively with the seven FLU-specific CD8$^+$ T-cell signatures (Supplementary Fig. S2B). Cluster analysis thus confirmed that gp100-specific memory/effector CD8$^+$ T cells had phenotype signatures which were not unique, but were closely homologous to the distinct signatures of either CMV-specific or FLU-specific T cells.

Discussion

Data presented herein show that the frequencies of long-term memory CD8$^+$ T cells specific for the self-tumor antigen, gp100, in 16 disease-free patients, previously vaccinated with gp100$_{209\text{-}2M}$, were comparable with the frequencies of memory CD8$^+$ T cells specific for the viral antigens CMV (pp65) and FLU (MI) detected in the same patients, suggesting homeostasis-driven proliferation of gp100-specific memory T cells. This conclusion is supported by the detection of high levels of CD127 on gp100-specific long-term memory and boosted T cells in some patients (data not shown). Boosted patients exhibited an anamnestic response shown by the significantly increased mean frequency of circulating gp100-specific T cells over corresponding long-term memory values for 12 of 16 patients after two boosting immunizations. By comparison, four to six repetitive vaccines given at 2-week to 3-week intervals were required in the initial priming vaccine regimen to stimulate even marginal frequencies of gp100-specific T cells. However, the mean frequency of peptide-specific CD8$^+$ T cells after boosting was statistically lower than the mean frequency measured after the initial series of immunizations and did not improve despite four to six more boosting vaccinations over 3 years (data not shown). This indicates that the boosted response was not robust enough to equal or exceed the response measured after primary immunization in most patients. However, data from infectious disease prime-boost immunization studies indicate circulating memory CD8$^+$ T cells are cleared from the blood within 3 to 4 weeks of immunization and rapidly traffic to peripheral organs (23, 48). Repetitive boosting also increases the rate of trafficking to nonlymphoid organs (23). After the second boosting immunization, the subsequent follow-up boosting vaccines and correlated blood draws in our study were 6 months apart. Thus, the failure to detect an increased frequency of circulating gp100-specific T cells may not reflect the true extent of the anamnestic response because trafficking of antigen-specific T cells to peripheral organs during the 6 months between immunizations could significantly reduce circulating levels of memory T cells.

Even in the absence of high numbers of circulating memory T cells, competent memory T-cell differentiation could still be reflected by enhanced functional responses because memory T cells have increased functional avidity and proliferation potential, as well as heightened cytokine responses after

Downloaded from http://aacrjournals.org/clincancerres/article-pdf/14/16/5270/1975801/5270.pdf by guest on 09 December 2023

secondary antigen stimulation (reviewed in ref. 30). Our patients exhibited no improvement in the functional avidity of long-term memory or boosted IVS T cells compared with the T-cell response measured after the initial vaccine regimen. *In vitro* stimulation of $gp100_{209\text{-}2M}$ IVS cells from all three time points with an $A2^+/gp100^+$ tumor cell line (Mel 118) showed there was no increase in the mean frequency of degranulating $CD107^+$ gp100-specific $CD8^+$ T cells in the long-term memory or boosted cells compared with T cells at the completion of the initial adjuvant trial, suggesting that neither long-term memory nor boosted cells exhibited increased $gp100^+$ tumor cell-specific CTL function. Additional statistical subanalysis showed there was no significant difference between patients with the FLU-like versus CMV-like phenotypes with regard to the functional avidity of LTM ($P = 0.66$) or P2B (0.49) T cells. Similarly, there was no statistical difference in the LTM ($P = 0.79$) or P2B ($P = 0.68$) CD107 responses of T cells with the two phenotypes. By comparison, *in vitro* proliferation responses to cognate peptide at all time points for most patients were ≥10-fold higher than their respective *ex vivo* values. This was particularly true for long-term memory T cells which achieved increases (range, 50-242 fold) that were higher than those of either postadjuvant vaccine or boosted T cells in 8 of 16 patients. Notably, subanalysis using an unpaired *t* test indicated that gp100-specific LTM T cells with a FLU-like signature exhibited a significant ($P = 0.0211$) mean increase in *in vitro* proliferation compared with memory cells with a CMV-like signature. Memory T cells have a much reduced lag time from activation to cell cycle entry compared with naive cells, because they contain preformed cytoplasmic cyclin D3/cyclin-dependent kinase 6 complexes that maintain the cells in a late G_1 phase (30, 49). This "ready-to-go" status facilitates rapid S-phase transition after reactivation (30, 49). Memory T cells not only divide more rapidly, but they also have a largely unexplained ability to survive the massive cell death that frequently occurs *in vivo* during the expansion phase of the immune response and also after IVS (30). The average six-fold increase in the *in vivo* frequencies of boosted circulating gp100-specific T cells over long-term memory T-cell frequencies and the high *in vitro* proliferation responses of long-term memory $CD8^+$ T cells compared with the absence of heightened functional responses in these cells may indicate that the proliferation of memory T cells is regulated by different mechanisms than those governing effector functions and represents a separate control point for memory $CD8^+$ T-cell differentiation (50). Thus, repetitive class I peptide immunization in the absence of exogenous T_h antigens seemed to result in circulating long-term memory T cells with increased potential for *in vivo* and *in vitro* proliferation after peptide rechallenge, but without the enhanced functional properties of fully competent memory T cells.

The inability to boost the frequency of $gp100^+/CD8^+$ T cells to levels achieved after the initial series of vaccines could also be attributable to tolerogenic mechanisms mediated by increased regulatory T cells (51), myeloid suppressor cells (52), or increased expression of $PD\text{-}1^+/CD8^+$ T cells (53). Although we have not studied myeloid suppressor cells, the frequency of $PD\text{-}1^+$ gp100-specific T cells was comparable with those of CMV-specific and FLU-specific memory T cells in the same patients (data not shown). Regulatory T-cell frequencies in individual patients varied from 2.5% to 9% and were not higher among long-term memory or boosted T cells than in prevaccine and PIVR PBMCs (data not shown). Although not conclusive, these data suggested the limited anamnestic responses in some patients were not strictly due to immune suppression, but might also reflect alteration of intrinsic $CD8^+$ memory T-cell function—possibly due to inadequate $CD4^+$ T_h cells at priming. Effective priming of $CD8^+$ T cells in the presence of T_h cells results in DNA changes that improve the transcription of certain genes (54). Examples include the permanent and heritable demethylation of the IFN-γ locus in memory $CD8^+$ T cells (55) and the demethylation of the IL-4 gene in Th_2 $CD4^+$ memory T cells (56). These permanent modifications are thought to be regulated by the expression of T-box transcription factors, such as T-bet and eomesodermin in memory $CD8^+$ cells, and may be altered in the absence of $CD4^+$ helper T cells (57, 58). Memory $CD8^+$ T cells generated in the absence of $CD4^+$ T_h cells (so-called "lethargic" cells), die upon reactivation with cognate antigen due to the up-regulated expression of tumor necrosis factor–related apoptosis-inducing ligand, which is not expressed in competent memory T cells (59). Analysis of T-box transcription factor mRNA synthesis and tumor necrosis factor–related apoptosis-inducing ligand expression by long-term gp100-specific memory T cells has recently been initiated at our institute to determine if they are quantitatively different from those of competent memory T cells specific for CMV or FLU in the same patients.

Higher order polychromatic flow cytometry analysis of normal human $CD8^+$ T cells has recently been done using simultaneous staining with multiple antibodies specific for key cell surface markers and for perforin (Per), granzyme A (GraA), and granzyme B (GraB; refs. 35, 36). These studies suggested the following $CD8^+$ T-cell differentiation pathway: early T_{EM} ($CCR7^-/CD45RA^-/CD27^+/CCR5^+/CD28^+/Per^{-/low}/GraA^+/GraB^-$) → late T_{EM} ($CCR7^-/CD45RA^-/CD27^{low}/CCR5^{low}/CD28^-/Per^{low}/GraA^+/GraB^+$) → effector ($CCR7^-/D45RA^{+/-}/CD27^-/CCR5^{low/-}/CD28^-/Per^+/GraA^+/GraB^+$). The sequential expression of the cytolytic molecules correlated with the concomitant loss of CD28, CD27, and CCR5 expression and was the basis for the definitions of "early" and "late" T_{EM} and effector $CD8^+$ T-cell phenotypes. In a similar analysis, Romero et al. (60) described five major subphenotypes of normal human $CD8^+$ T cells: CM ($CD45RA^-/CCR7^+/CD27^+/CD28^+$), EM_1 ($CD45RA^-/CCR7^-/CD27^+/CD28^+$), EM_2 ($CD45RA^-/CCR7^-/CD27^+/CD28^-$), EM_3 ($CD45RA^-/CCR7^-/CD27^-/CD28^-$), and EM_4 ($CD45RA^-/CCR7^-/CD27^-/CD28^+$). EM_1 and EM_4 subphenotypes were very similar, and PCR analysis of sorted cells showed that, like CM T cells, they exhibited low levels of granzyme B and perforin, high levels of CD127/IL-7Rα, and long telomeres, suggesting a short replication history—all characteristics of memory T cells. By comparison, PCR analysis of sorted EM_2 and EM_3 T cells revealed elevated levels of granzyme B and perforin, minimal CD127 expression, and shorter telomeres, indicating more cycles of cell division–all characteristic traits of effector $CD8^+$ T cells. EM_3 cells also displayed CTL function comparable with fully differentiated effector T cells (60). The CM and EM_1/EM_4 subpopulations are very similar to the gp100-specific T_{CM} and early T_{EM} subphenotypes, respectively, and the terminal effector and EM_2/EM_3 T-cell subphenotypes seem very homologous to the T_{RVE} $CD8^+$ T-cell subpopulations described herein. Romero and coworkers further suggested that the up-regulation of cytolytic mediators and the apparent stepwise loss of CCR7, CD27, and CD28 indicated a progressive differentiation from

Downloaded from http://aacrjournals.org/clincancerres/article-pdf/14/16/5270/1975801/5270.pdf by guest on 09 December 2023

memory cells (EM_1/EM_4) to effector cells (EM_2/EM_3/terminal effectors; ref. 60). The similarity of the gp100-specific $CD8^+$ T cells described in our study to the putative memory and effector subpopulations recently described in antigen nonspecific normal human T cells and the close homology of the gp100-specific T-cell phenotypes to those of CMV-specific and FLU-specific $CD8^+$ T cells indicates that self-tumor antigen-specific memory $CD8^+$ T cells exhibit conventional phenotypes.

It is tempting to assume that the T_{RVE}-rich, gp100-specific $CD8^+$ T-cell signatures of patients EA02, EA07, and EA29 indicate they may be responding to chronic antigen activation, as might occur with micrometastatic disease or from autoimmune stimulation. T_{CM}/T_{EM}-rich, FLU-like gp100-specific signatures of patients EA19, EA12, EA28, and EA35 might therefore conversely suggest the maintenance of competent resting memory T cells after the complete clearance of melanoma tumor antigen. However, this interpretation is not supported by other published data. CMV-specific, T_{RVE}-like $CD8^+$ T cells are maintained long-term in seropositive individuals and have long telomeres and increased telomerase activity, which may explain their memory-like maintenance (15, 47, 61, 62). Analysis of CMV-specific $CD8^+$ T cells in rhesus macaques strongly suggests that $CD28^-$ effector-memory T cells retain replication potential and are sustained by independent homeostasis-driven mechanisms comparable with those that maintain central memory $CD8^+$ T-cell levels (63). Homeostasis of CMV-specific effector-memory or T_{RVE}-like T cells may not depend on IL-7, because chronic viral infection down-regulates IL-7Rα (CD127) on antigen-specific T cells (15, 64). Other data suggest the dominant T_{CM} and T_{EM} subpopulations that characterize some gp100-specific $CD8^+$ T-cell memory responses may not be unique to the clearance of an acute antigen challenge because they are also detected at high frequencies in the memory T-cell response to chronic infections with EBV and HCV (65). Moreover, increased tumor burden in melanoma patients has been correlated with the increased presence of tumor-specific $CD8^+$ T cells exhibiting a very early resting memory phenotype ($CCR7^+/CD45RA^+/CD27^+/CD28^+/perforin^-$) in tumor-invaded lymph nodes. This was also correlated with the absence of tumor regression in metastatic lesions (66). Thus, the expression of memory (T_{CM}/T_{EM}) subpopulations of circulating $CD8^+$ T cells without concomitant effector T cells may reflect the influence of tolerogenic/suppressive down-regulation of effector T-cell differentiation rather than the potential for fully competent memory T-cell proliferative and functional activation. This notion is also supported by a recent study that showed that the dominant CEA, MAGE, and HER-2/neu-specific $CD8^+$ T cells detected in nonimmunized metastatic breast cancer patients exhibited early T_{EM}-like phenotypes (i.e., $CD45RA^-/CD27^{+/-}/CD28^+$) and exhibited high levels of IL-2 expression compared with CMV-specific or FLU-specific T cells in the same patients (67). Whereas IL-2 expression is characteristic of memory T cells, the highly restricted tumor-associated antigen–specific memory phenotype and the correlated absence of IFN-γ^+ or tumor necrosis factor-α^+ T cells compared with CMV-specific or FLU-specific T cells suggested impaired tumor-associated antigen–specific protective immunity in these patients (67). The authors argued that the heightened IL-2 expression by tumor antigen–specific memory T cells may actually contribute to immunologic quiescence through the up-regulation of T regulatory cells. Taken together, these data suggest that a phenotype signature rich in terminal-effector or T_{RVE} subphenotypes, similar to that commonly found in CMV^+ donors, could indicate the homeostasis-driven maintenance of a memory T-cell component capable of self-replication. The data similarly support the concept that a T_{CM}/T_{EM}-rich resting memory T-cell signature like that found after the clearance of an acute viral challenge could reflect a state of immunologic anergy rather than anamnestic potential if tolerogenic forces are in play. Notably, our study indicated there was no statistical difference in functional avidity or CD107 mobilization exhibited by gp100-specific IVS $CD8^+$ T cells from patients expressing the two major phenotypes. By contrast, there was a significantly higher peptide-stimulated *in vitro* proliferation response of memory T cells with the FLU-like signature. However, the clinical significance of this observation is unclear at present because there was no clinical correlation with either subphenotype signature, and there was no evidence of vitiligo in any patient. Moreover, both the CMV-like and FLU-like phenotype signatures were observed with equal frequency in the four booster patients who have subsequently developed progressive disease (data not shown). At present, the biological/clinical significance of these phenotype differences in our study remains unresolved. Future clinical trials with much larger patient enrollment may provide the statistical power to determine if there is diagnostic/prognostic relevance to the two distinct self-tumor antigen-specific memory T-cell phenotype signatures.

In conclusion, these data show that even in otherwise healthy disease-free melanoma patients, the therapeutic vaccine strategy used did not induce fully competent gp100-specific memory $CD8^+$ T cells. The data presented suggest that whereas repetitive class I–restricted melanoma peptide vaccination by itself can break tolerance to self-tumor antigens, other vaccine strategies will be required to induce functionally competent long-term memory T cells capable of robust anamnestic response to tumor challenge.

Disclosure of Potential Conflicts of Interest

No potential conflict of interest were disclosed.

Acknowledgments

We thank Dr. Andrew Weinberg and Dr. Nora Disis for reviewing the manuscript, Tanisha Meeuwsen and Iliana Gonzalez for their technical assistance, Molly Torgeson for her excellent assistance in preparation of the article, and the Cancer Therapy Evaluation Program for providing the gp100209-2M peptide (NSC 683472) and Montanide ISA 51 for our study.

References

1. Rosenberg SA, Yang JC, Schwartzentruber DJ, et al. Immunologic and therapeutic evaluation of a synthetic peptide vaccine for the treatment of patients with metastatic melanoma. Nat Med 1998;4:321–7.
2. Rosenberg SA, Sherry RM, Morton KE, et al. Tumor progression can occur despite the induction of very high levels of self/tumor antigen-specific CD8+ T cells in patients with melanoma. J Immunol 2005;175:6169–76.
3. Ayyoub M, Zippelius A, Pittet MJ, et al. Activation of human melanoma reactive CD8+ T cells by vaccination with an immunogenic peptide analog derived from Melan-A/melanoma antigen recognized by T cells-1. Clin Cancer Res 2003;9:669–77.
4. Speiser DE, Romero P. Toward improved immuno-

Downloaded from http://aacrjournals.org/clincancerres/article-pdf/14/16/5270/1975801/5270.pdf by guest on 09 December 2023

competence of adoptively transferred CD8+ T cells. J Clin Invest 2005;115:1467–9.
5. Boon T, Coulie PG, Van den Eynde BJ, van der Bruggen P. Human T cell responses against melanoma. Annu Rev Immunol 2006;24:175–208.
6. Rosenberg SA, Yang JC, Restifo NP. Cancer immunotherapy: moving beyond current vaccines. Nat Med 2004;10:909–15.
7. Klebanoff CA, Gattinoni L, Torabi-Parizi P, et al. Central memory self/tumor-reactive CD8+ T cells confer superior antitumor immunity compared with effector memory T cells. Proc Natl Acad Sci U S A 2005;102:9571–6.
8. Roberts AD, Ely KH, Woodland DL. Differential contributions of central and effector memory T cells to recall responses. J Exp Med 2005;202:123–33.
9. Klebanoff CA, Gattinoni L, Restifo NP. CD8+ T-cell memory in tumor immunology and immunotherapy. Immunol Rev 2006;211:214–24.
10. Powell DJ, Jr., Rosenberg SA. Phenotypic and functional maturation of tumor antigen-reactive CD8+ T lymphocytes in patients undergoing multiple course peptide vaccination. J Immunother 2004;27:36–47.
11. Smith JW II, Walker EB, Fox BA, et al. Adjuvant immunization of HLA-A2-positive melanoma patients with a modified gp100 peptide induces peptide-specific CD8+ T-cell responses. J Clin Oncol 2003;21:1562–73.
12. Walker EB, Haley D, Miller W, et al. gp100(209-2M) peptide immunization of human lymphocyte antigen-A2+ stage I-III melanoma patients induces significant increase in antigen-specific effector and long-term memory CD8+ T cells. Clin Cancer Res 2004;10:668–80.
13. Champagne P, Ogg GS, King AS, et al. Skewed maturation of memory HIV-specific CD8 T lymphocytes. Nature 2001;410:106–11.
14. Kuijpers TW, Vossen MT, Gent MR, et al. Frequencies of circulating cytolytic, CD45RA+CD27-, CD8+ T lymphocytes depend on infection with CMV. J Immunol 2003;170:4342–8.
15. van Leeuwen EM, de Bree GJ, ten Berge IJ, van Lier RA. Human virus-specific CD8+ T cells: diversity specialists. Immunol Rev 2006;211:225–35.
16. Meijer SL, Dols A, Jensen SM, et al. Induction of circulating tumor-reactive CD8+ T cells after vaccination of melanoma patients with the gp100 209-2M peptide. J Immunother 2007;30:533–43.
17. Perfetto SP, Chattopadhyay PK, Roederer M. Seventeen-colour flow cytometry: unravelling the immune system. Nat Rev Immunol 2004;4:648–55.
18. Bagwell CB. Hyperlog-a flexible log-like transform for negative, zero, and positive valued data. Cytometry A 2005;64:34–42.
19. Petrausch U, Haley D, Miller W, et al. Polychromatic flow cytometry: a rapid method for the reduction and analysis of complex multiparameter data. Cytometry A 2006;69:1162–73.
20. Tung JW, Parks DR, Moore WA, Herzenberg LA. New approaches to fluorescence compensation and visualization of FACS data. Clin Immunol 2004;110:277–83.
21. Saeed AI, Sharov V, White J, et al. TM4: a free, open-source system for microarray data management and analysis. Biotechniques 2003;34:374–8.
22. Gentleman RC, Carey VJ, Bates DM, et al. Bioconductor: open software development for computational biology and bioinformatics. Genome Biol 2004;5:R80.
23. Masopust D, Ha SJ, Vezys V, Ahmed R. Stimulation history dictates memory CD8 T cell phenotype: implications for prime-boost vaccination. J Immunol 2006;177:831–9.
24. Busch DH, Pamer EG. T cell affinity maturation by selective expansion during infection. J Exp Med 1999;189:701–10.
25. Kedl RM, Schaefer BC, Kappler JW, Marrack P. T cells down-modulate peptide-MHC complexes on APCs *in vivo*. Nat Immunol 2002;3:27–32.
26. Rodriguez F, Harkins S, Slifka MK, Whitton JL. Immunodominance in virus-induced CD8(+) T-cell responses is dramatically modified by DNA immunization and is regulated by γ interferon. J Virol 2002;76:4251–9.
27. Slifka MK, Whitton JL. Functional avidity maturation of CD8(+) T cells without selection of higher affinity TCR. Nat Immunol 2001;2:711–7.
28. Cawthon AG, Alexander-Miller MA. Optimal colocalization of TCR and CD8 as a novel mechanism for the control of functional avidity. J Immunol 2002;169:3492–8.
29. Veiga-Fernandes H, Walter U, Bourgeois C, McLean A, Rocha B. Response of naive and memory CD8+ T cells to antigen stimulation *in vivo*. Nat Immunol 2000;1:47–53.
30. Rocha B, Tanchot C. The Tower of Babel of CD8+ T-cell memory: known facts, deserted roads, muddy waters, and possible dead ends. Immunol Rev 2006;211:182–96.
31. Betts MR, Brenchley JM, Price DA, et al. Sensitive and viable identification of antigen-specific CD8+ T cells by a flow cytometric assay for degranulation. J Immunol Methods 2003;281:65–78.
32. van Baarle D, Kostense S, van Oers MH, Hamann D, Miedema F. Failing immune control as a result of impaired CD8+ T-cell maturation: CD27 might provide a clue. Trends Immunol 2002;23:586–91.
33. Kern F, Khatamzas E, Surel I, et al. Distribution of human CMV-specific memory T cells among the CD8pos. Subsets defined by CD57, CD27, and CD45 isoforms. Eur J Immunol 1999;29:2908–15.
34. Geginat J, Lanzavecchia A, Sallusto F. Proliferation and differentiation potential of human CD8+ memory T-cell subsets in response to antigen or homeostatic cytokines. Blood 2003;101:4260–6.
35. Tomiyama H, Matsuda T, Takiguchi M. Differentiation of human CD8(+) T cells from a memory to memory/effector phenotype. J Immunol 2002;168:5538–50.
36. Takata H, Takiguchi M. Three memory subsets of human CD8+ T cells differently expressing three cytolytic effector molecules. J Immunol 2006;177:4330–40.
37. Sallusto F, Lenig D, Forster R, Lipp M, Lanzavecchia A. Two subsets of memory T lymphocytes with distinct homing potentials and effector functions. Nature 1999;401:708–12.
38. Brenchley JM, Karandikar NJ, Betts MR, et al. Expression of CD57 defines replicative senescence and antigen-induced apoptotic death of CD8+ T cells. Blood 2003;101:2711–20.
39. Faint JM, Annels NE, Curnow SJ, et al. Memory T cells constitute a subset of the human CD8+CD45RA+ pool with distinct phenotypic and migratory characteristics. J Immunol 2001;167:212–20.
40. Khan N, Shariff N, Cobbold M, et al. Cytomegalovirus seropositivity drives the CD8 T cell repertoire toward greater clonality in healthy elderly individuals. J Immunol 2002;169:1984–92.
41. Chen G, Shankar P, Lange C, et al. CD8 T cells specific for human immunodeficiency virus, Epstein-Barr virus, and cytomegalovirus lack molecules for homing to lymphoid sites of infection. Blood 2001;98:156–64.
42. Wherry EJ, Teichgraber V, Becker TC, et al. Lineage relationship and protective immunity of memory CD8 T cell subsets. Nat Immunol 2003;4:225–34.
43. Marzo AL, Klonowski KD, Le Bon A, et al. Initial T cell frequency dictates memory CD8+ T cell lineage commitment. Nat Immunol 2005;6:793–9.
44. van Faassen H, Saldanha M, Gilbertson D, et al. Reducing the stimulation of CD8+ T cells during infection with intracellular bacteria promotes differentiation primarily into a central (CD62LhighCD44high) subset. J Immunol 2005;174:5341–50.
45. de Bree GJ, Heidema J, van Leeuwen EM, et al. Respiratory syncytial virus-specific CD8+ memory T cell responses in elderly persons. J Infect Dis 2005;191:1710–8.
46. He XS, Mahmood K, Maecker HT, et al. Analysis of the frequencies and of the memory T cell phenotypes of human CD8+ T cells specific for influenza A viruses. J Infect Dis 2003;187:1075–84.
47. Wallace DL, Zhang Y, Ghattas H, et al. Direct measurement of T cell subset kinetics *in vivo* in elderly men and women. J Immunol 2004;173:1787–94.
48. Bachmann MF, Wolint P, Schwarz K, Jager P, Oxenius A. Functional properties and lineage relationship of CD8+ T cell subsets identified by expression of IL-7 receptor α and CD62L. J Immunol 2005;175:4686–96.
49. Veiga-Fernandes H, Rocha B. High expression of active CDK6 in the cytoplasm of CD8 memory cells favors rapid division. Nat Immunol 2004;5:31–7.
50. Hernandez J, Aung S, Marquardt K, Sherman LA. Uncoupling of proliferative potential and gain of effector function by CD8(+) T cells responding to self-antigens. J Exp Med 2002;196:323–33.
51. Sakaguchi S. Naturally arising Foxp3-expressing CD25+CD4+ regulatory T cells in immunological tolerance to self and non-self. Nat Immunol 2005;6:345–52.
52. Pollard JW. Tumour-educated macrophages promote tumour progression and metastasis. Nat Rev Cancer 2004;4:71–8.
53. Barber DL, Wherry EJ, Masopust D, et al. Restoring function in exhausted CD8 T cells during chronic viral infection. Nature 2006;439:682–7.
54. Agarwal S, Rao A. Modulation of chromatin structure regulates cytokine gene expression during T cell differentiation. Immunity 1998;9:765–75.
55. Fitzpatrick DR, Shirley KM, Kelso A. Cutting edge: stable epigenetic inheritance of regional IFN-γ promoter demethylation in CD44highCD8+ T lymphocytes. J Immunol 1999;162:5053–7.
56. Ouyang W, Lohning M, Gao Z, et al. Stat6-independent GATA-3 autoactivation directs IL-4-independent Th2 development and commitment. Immunity 2000;12:27–37.
57. Pearce EL, Mullen AC, Martins GA, et al. Control of effector CD8+ T cell function by the transcription factor Eomesodermin. Science 2003;302:1041–3.
58. Intlekofer AM, Takemoto N, Wherry EJ, et al. Effector and memory CD8+ T cell fate coupled by T-bet and eomesodermin. Nat Immunol 2005;6:1236–44.
59. Janssen EM, Droin NM, Lemmens EE, et al. CD4+ T-cell help controls CD8+ T-cell memory via TRAIL-mediated activation-induced cell death. Nature 2005;434:88–93.
60. Romero P, Zippelius A, Kurth I, et al. Four functionally distinct populations of human effector-memory CD8+ T lymphocytes. J Immunol 2007;178:4112–9.
61. Hathcock KS, Kaech SM, Ahmed R, Hodes RJ. Induction of telomerase activity and maintenance of telomere length in virus-specific effector and memory CD8+ T cells. J Immunol 2003;170:147–52.
62. Hamann D, Kostense S, Wolthers KC, et al. Evidence that human CD8+CD45RA+CD27- cells are induced by antigen and evolve through extensive rounds of division. Int Immunol 1999;11:1027–33.
63. Pitcher CJ, Hagen SI, Walker JM, et al. Development and homeostasis of T cell memory in rhesus macaque. J Immunol 2002;168:29–43.
64. Wherry EJ, Barber DL, Kaech SM, Blattman JN, Ahmed R. Antigen-independent memory CD8 T cells do not develop during chronic viral infection. Proc Natl Acad Sci U S A 2004;101:16004–9.
65. Appay V, Dunbar PR, Callan M, et al. Memory CD8+ T cells vary in differentiation phenotype in different persistent virus infections. Nat Med 2002;8:379–85.
66. Mortarini R, Piris A, Maurichi A, et al. Lack of terminally differentiated tumor-specific CD8+ T cells at tumor site in spite of antitumor immunity to self-antigens in human metastatic melanoma. Cancer Res 2003;63:2535–45.
67. Inokuma M, dela Rosa C, Schmitt C, et al. Functional T cell responses to tumor antigens in breast cancer patients have a distinct phenotype and cytokine signature. J Immunol 2007;179:2627–33.

Downloaded from http://aacrjournals.org/clincancerres/article-pdf/14/16/5270/1975801/5270.pdf by guest on 09 December 2023